Analysis of planar waveguides using Wentzel–Kramers–Brillouin–type methods

Article *in* Journal of Modern Optics · February 2004

DOI: 10.1080/09500340310001603177

CITATIONS
2

READS
138

5 authors, including:

Carlos R. Fernandez-Pousa
Universidad Miguel Hernández de Elche
120 PUBLICATIONS **1,007** CITATIONS

SEE PROFILE

M.T. Flores-Arias
University of Santiago de Compostela
144 PUBLICATIONS **511** CITATIONS

SEE PROFILE

Carmen Bao
University of Santiago de Compostela
121 PUBLICATIONS **468** CITATIONS

SEE PROFILE

JOURNAL OF MODERN OPTICS, 2003, 1–11, preview article

Analysis of planar waveguides using Wentzel–Kramers–Brillouin-type methods

C. R. FERNÁNDEZ-POUSA, F. MATEOS

Departamento de Ciencia y Tecnología de Materiales, Universidad Miguel Hernández de Elche, Avenida Ferrocarril s/n, E03202 Elche (Alicante), Spain; e-mail: c.pousa@umh.es

M. T. FLORES-ARIAS, C. BAO and M. V. PÉREZ

Laboratorio de Óptica, Departamento de Física Aplicada, Universidad de Santiago de Compostela, Campus Sur, E15782 Santiago de Compostela, Spain

(*Received 6 March 2003; revision received 10 July 2003*)

Abstract. A presentation of four different schemes of semiclassical or Wentzel–Kramers–Brillouin-type approximations to planar waveguides is given. Attention is paid to a recent proposal for mapping a general symmetric waveguide into the hyperbolic secant or symmetric Epstein profile by exploring the dispersion relation and the fundamental mode field. As a test, these approximations are compared with the series solution of the cladded-parabolic profile.

1. Introduction

Among the diversity of techniques to analyse planar gradient-index dielectric waveguides [1], the Wentzel–Kramers–Brillouin (WKB) or semiclassical method still is an approximate but simple procedure [2]. The main benefit of the method is its generality, since it is just the leading-order approximation to the exact solution of the modal equation in the geometrical limit. Thus, the WKB approximation can represent the starting point for other analysis of planar or rectangular waveguides, for instance using the effective-index method.

In the usual presentation of the WKB method [2], the modal equation of a planar waveguide is integrated using an expansion of the problem in the optical wavelength λ_0. The WKB method gives the solution up to second order. The solution is connected through turning points using the connection formulae. However, this point of view is equivalent to a special case of a more general formulation [3], called the Miller–Good or WKB-type transformation. There, a non-solvable profile is mapped into a solvable profile, which is assumed to model properly the global structure of the original problem. This mapping is constructed using nonlinear transformations relating both the modal field and the physical length of the waveguide. The WKB method itself is recovered by transforming a general profile into two solvable constant index profiles, before and after the turning points, using the connection formulae to join the modal fields in the different domains.

Journal of Modern Optics ISSN 0950–0340 print/ISSN 1362–3044 online
http://www.tandf.co.uk/journals
DOI: 10.1080/09500340310001603177

In [4], a new WKB-type method for one-dimensional profiles has been proposed. In this case, the solvable profile is the symmetric Epstein or hyperbolic secant. This general scheme has been applied in at least two other forms: mapping the original problem into the linear profile [5] or into the parabolic profile [3]. The aim of this work is to extend this proposal by setting it in a general framework, and to compare the WKB-type approximations by exploring both the dispersion relation (V–b plot), and the fundamental mode of a particular waveguide.

The plan of this paper is the following. In section 2 we reintroduce the method of Miller and Good so that we present all these WKB-type approximations in a unified structure. In section 3, we explore the three known implementations of the basic technique, which map a general problem into linear, parabolic or Epstein profiles. We also add to these three schemes the fourth simple solvable profile, namely the exponential profile. In section 4 we shall explore how these four schemes behave as the non-solvable profile, that is the cladded-parabolic profile, for which well-established numerical [6, 7] or semianalytical [8] techniques are known. This choice of profile will allow us to explore the consequences in these methods of the non-smoothness of the problem profile.

2. General scheme for Wentzel–Kramers–Brillouin-type methods

The WKB-type technique can be stated as follows. For clarity, we shall restrict our attention to symmetric profiles, although our considerations can be extended to asymmetric profiles along the lines of [9]. Let us consider a planar dielectric waveguide whose index profile in the transverse direction x is

$$n^2(x) = n_1^2 + \left(n_2^2 - n_1^2\right) f(x). \tag{1}$$

Here, n_1 is the refraction index of the core of the waveguide, and n_2 is the index of the cladding. The function $f(x)$ describes the index profile, and it is assumed to be continuous; symmetric, $f(x) = f(-x)$; normalized, $f(0) = 1$; null for large values of x, $f(x \to \infty) \to 0$. The wave equation that governs the propagation of the transverse electric modes is

$$\frac{\mathrm{d}^2 E}{\mathrm{d}x^2} + \left[k_0^2 n^2(x) - \beta^2\right] E(x) = 0, \tag{2}$$

where k_0 is the wavenumber in vacuum and β the propagation constant of the mode. We shall assume that equation (2) has a unique turning point that corresponds to a simple zero of the potential term in square brackets. As is well known, equation (2) can be expressed in adimensional form; since the refraction index is adimensional, the profile function $f(x)$ must contain a parameter a with dimensions of length, which can be chosen so that the normalized frequency is $V = k_0 a (n_1^2 - n_2^2)^{1/2}$. On the other hand, the normalized propagation constant is defined as $b = (\beta^2/k_0^2 - n_2^2)/(n_1^2 - n_2^2)$ and, with the definition of an adimensional transverse length $X = x/a$, equation (2) can be written in adimensional form as

$$\frac{\mathrm{d}^2 E}{\mathrm{d}X^2} + V^2 [f(X) - b] E(X) = 0. \tag{3}$$

This presentation is suitable when considering semiclassical approximations, since the geometrical optics limit is accomplished when $V \to \infty$. From now on, we shall substitute x for X in equation (3).

In general, equation (3) is not exactly solvable, but it can be mapped into a simpler problem by means of a transformation. Assume that a equation of the type

$$\frac{\mathrm{d}^2G}{\mathrm{d}y^2} + q^2(y)G(y) = 0 \tag{4}$$

can be integrated. To keep the physical picture, we shall represent the potential in equation (4) as an index profile from a solvable waveguide, $q^2(y) = \Lambda^2[g(y)-b]$ for certain values of the normalized frequency Λ and profile function $g(y)$. It is possible to relate equations (3) and (4) through [3]

$$E(x) = \frac{1}{[y'(x)]^{1/2}} G(y(x)), \tag{5}$$

where the prime denotes the derivative with respect to the argument. Substitution of equation (5) into equation (3) and using equation (4) result in a condition on $y(x)$:

$$[y'(x)]^{1/2} \frac{\mathrm{d}^2}{\mathrm{d}x^2} \frac{1}{[y'(x)]^{1/2}} + V^2[f(x) - b] - \Lambda^2[g(y(x)) - b]y'(x)^2 = 0. \tag{6}$$

Neglecting the second derivative with respect to x, then the function $y(x)$ can be integrated to

$$V \int^x [f(x) - b]^{1/2} \mathrm{d}x = \Lambda \int^y [g(y) - b]^{1/2} \mathrm{d}y. \tag{7}$$

This approximation can be justified in two ways: firstly, since the function $y(x)$ is defined implicitly in an integral, it can be assumed to be slowly varying [9, 10]; secondly, since $V \simeq \Lambda \to \infty$ in the geometrical limit $\lambda_0 \to 0$ and the second derivative contains no V parameter, this approximation is equivalent to the semiclassical approximation [3]. Both points of view reflect the fact that the function $[y'(x)]^{-1/2}$ is assumed to be a slowly varying envelope of the field $G(y(x))$ in equation (5).

Equation (7) will be used to define a transformation of the region $x \geq 0$ into $y(x) \geq 0$ mapping two concrete points x_0 and y_0 into each other. It is customary to choose x_0 and y_0 as the turning points of the two profiles ($f(x_0) = b, g(y_0) = b$), since in those values the modal fields change from an oscillatory to a decaying behaviour. Then, the complete definition of the transformation is

$$V \int_x^{x_0} [f(x) - b]^{1/2} \mathrm{d}x = \Lambda \int_y^{y_0} [g(y) - b]^{1/2} \mathrm{d}y, \tag{8}$$

$$V \int_{x_0}^x [b - f(x)]^{1/2} \mathrm{d}x = \Lambda \int_{y_0}^y [b - g(y)]^{1/2} \mathrm{d}y, \tag{9}$$

before and after the turning points respectively. Thus, to map the domain $x \geq 0$ into $y(x) \geq 0$ it is necessary that

$$V \int_0^{x_0} [f(x) - b]^{1/2} \mathrm{d}x = \Lambda \int_0^{y_0} [g(y) - b]^{1/2} \mathrm{d}y \tag{10}$$

which is the definition of the Λ parameter in terms of V. The resulting transformed equation is

$$\frac{\mathrm{d}^2 G}{\mathrm{d}y^2} + \left(\Lambda^2 [g(y) - b] - [y'(x)]^{1/2} \frac{\mathrm{d}^2}{\mathrm{d}y^2} \frac{1}{[y'(x)]^{1/2}} \right) G(y) = 0, \tag{11}$$

and therefore the original problem (3) can be integrated approximately by equation (4) if we neglect the contribution of the last term in parantheses in equation (11). This second derivative represents the error of the WKB-type approximation and can be neglected using the same type of arguments as in equation (7).

Transformation (8) and (9) is not only continuous by virtue of equation (10) but also differentiable. Expanding equations (8) and (9) in a series around x_0, it is easy to show that [3]

$$y'(x_0) = \left(\frac{V^2 f'(x_0)}{\Lambda^2 g'(y_0)} \right)^{1/3}, \tag{12}$$

and then the approximate solution (5) will not be singular at the turning points provided that y_0 corresponds also to a zero of first order.

3. Implementations of Wentzel–Kramers–Brillouin-type methods

In the first method to implement this procedure [3], $g(y)$ is parabolic: $g(y) = 1 - y^2$. The turning point $x = x_0$ of the general profile $f(x)$ is mapped into the turning point of the parabolic profile, $y = (1-b)^{1/2}$. The relation between normalized frequencies, according to equation (10), is

$$V \int_0^{x_0} [f(x) - b]^{1/2} \mathrm{d}x = \Lambda \frac{\pi}{4} (1 - b). \tag{13}$$

The modal fields are given by equation (5), where $G(y)$ are Hermite–Gauss functions. Explicitly, the fundamental mode is Gaussian like:

$$E_{\mathrm{P}}(x) = \frac{\text{constant}}{[y'(x)]^{1/2}} \exp\left(-\frac{y(x)^2}{2} \right). \tag{14}$$

Normalizability of the solutions implies that $\Lambda(1-b) = 2m+1$ ($m = 0, 1, 2, \ldots$), as is the case for the parabolic profile, and then equation (13) coincides with the dispersion relation of the usual WKB method. Although stated in a different way, this method is well known in quantum mechanics [11], and it represents an alternative proof of the WKB formula. It also justifies why the WKB approximation to the dispersion relation of the parabolic profile is exact.

Another method to create solutions of the wave equation (3) is due to Langer [5], and it was reintroduced by Ghatak and co-workers [9, 10]. The target profile $g(y)$ is now a linear function, $g(y) = 1 - y$, and then equation (10) is

$$V \int_0^{x_0} [f(x) - b]^{1/2} \mathrm{d}x = \Lambda \frac{2}{3} (1 - b)^{3/2}. \tag{15}$$

The resulting equation is integrated in $x \geq 0$ for bounded fields using the Airy function Ai [12]. The modes are of the form

$$E_{\mathrm{L}}(x) = \frac{\text{constant}}{[y'(x)]^{1/2}} Ai[\Lambda^{2/3}(y(x) + b - 1)]. \tag{16}$$

The dispersion relations for symmetric modes are obtained by requiring that the derivative of the field vanishes at $x = 0$, $dE_L/dx(0) = 0$, and the condition $E_L(0) = 0$ for antisymmetric modes. Using equation (15) this results in

$$\frac{Ai'\left[\Lambda^{2/3}(b-1)\right]}{Ai\left[\Lambda^{2/3}(b-1)\right]} = \frac{1}{2\Lambda^{2/3}}\frac{y''(0)}{[y'(0)]^2}, \qquad Ai\left[\Lambda^{2/3}(b-1)\right] = 0, \tag{17}$$

for symmetric and antisymmetric modes respectively.

The method proposed in [3] maps the original profile into a hyperbolic secant or Epstein symmetric profile [1, 7], $g(y) = \operatorname{sech}^2(y)$, transforming the turning point $x = x_0$ into $y = \operatorname{sech}^{-1}(b^{1/2})$. The new Λ parameter is defined through

$$V\int_0^{x_0}[f(x)-b]^{1/2}dx = \Lambda\frac{\pi}{2}\left(1-b^{1/2}\right). \tag{18}$$

The fundamental mode field in this scheme is

$$E_{HS}(x) = \frac{\text{constant}}{[y'(x)]^{1/2}}\cosh\left\{[y(x)]^{-\Lambda b^{1/2}}\right\}, \tag{19}$$

and the dispersion relation for the m mode ($m = 0, 1, 2, \ldots$), obtained as in the first case by requiring the normalizability of the fields, is simply the Λ–b formula for the symmetric Epstein model:

$$b = \frac{1}{4\Lambda^2}\left[2m+1-\left(4\Lambda^2+1\right)^{1/2}\right]^2. \tag{20}$$

Finally, we use as target profile the exponential profile [7, 13], $g(y) = \exp(-y)$, with turning point at $y_0 = -\ln b$. The relation between normalized frequencies is

$$V\int_0^{x_0}[f(x)-b]^{1/2}dx = 2\Lambda\left[(1-b)^{1/2} - b^{1/2}\cos^{-1}\left(b^{1/2}\right)\right]. \tag{21}$$

The modal fields in this scheme are of the form

$$E_{EXP}(x) = \frac{\text{constant}}{[y'(x)]^{1/2}}J_{2\Lambda b^{1/2}}\left[2\Lambda\exp\left(-\frac{y(x)}{2}\right)\right], \tag{22}$$

where $J_\nu(x)$ are the Bessel functions of the first kind and order ν [12]. As in the linear profile, the spectrum of normalizable solutions is continuous, and therefore the modes are obtained by requiring that $dE_{EXP}/dx(0) = 0$ for symmetric modes or $E_{EXP}(0) = 0$ for antisymmetric modes. This implies the following dispersion relations:

$$\frac{J'_{2\Lambda b^{1/2}}(2\Lambda)}{J_{2\Lambda b^{1/2}}(2\Lambda)} = -\frac{1}{2\Lambda}\frac{y''(0)}{[y'(0)]^2}, \qquad J_{2\Lambda b^{1/2}}(2\Lambda) = 0 \tag{23}$$

respectively.

4. A comparative example

In order to compare these four methods, we have analysed the cladded-parabolic profile $f(x) = 1 - x^2$ for $|x| < 1$ and zero otherwise. The parabolic mapping of Miller and Good implies that $V = \Lambda$ in equation (13), since both profiles are equal before the turning points. Moreover, the linear mapping sets

$\Lambda = V(3\pi/8)(1-b)^{-1/2}$ from equation (15), the hyperbolic secant mapping sets $\Lambda = V(1+b^{1/2})/2$ from equation (18), and the exponential mapping imply that

$$\Lambda = V\frac{\pi}{8}(1-b)\left[(1-b)^{1/2} - b^{1/2}\cos^{-1}\left(b^{1/2}\right)\right]^{-1} \tag{24}$$

from equation (21). Dispersion curves for the parabolic and hyperbolic secant profiles can be evaluated straightforwardly. Equations (17) for the linear profile reduces to

$$\frac{Ai'(\xi)}{Ai(\xi)} = -\frac{1}{4\xi}, \qquad Ai(\xi) = 0, \tag{25}$$

where $\xi = -\Lambda^{2/3}(1-b)$. Finally, equation (23), containing the dispersion relation in the exponential case, reduces to

$$\frac{J_{\nu+1}(\alpha) - J_{\nu-1}(\alpha)}{J_\nu(\alpha)} = \frac{\alpha}{\alpha^2 - \nu^2}, \qquad J_\nu(\alpha) = 0, \tag{26}$$

where $\alpha = 2\Lambda$ and $\nu = 2\Lambda b^{1/2}$ for symmetric and antisymmetric modes respectively, and we have used in the former the well-known relation for the derivatives of the Bessel functions.

In order to check these four approaches for the cladded-parabolic profile, we have computed its series solutions presented in [6] with 20 coefficients. This is considered as our exact solution. Numerical solutions for equations (25) and (26) are obtained with the MATLAB implementation of the Levenberg–Marquardt algorithm.

In figure 1 we show the resulting V–b curves for these four schemes and for the series solution. We observe that for all modes the approximations coincide in the geometrical limit. Moreover, linear and exponential schemes give similar results. The main differences in the curves occur in the fundamental mode, where neither linear nor exponential mappings yield accurate results. The hyperbolic secant is a good approximation near the cut-off, since it is the only guide that reproduces the threshold $b = 0$ for the fundamental mode. It could seem strange that the exponential approximation, a profile whose fundamental mode cut-off is also zero as the hyperbolic secant, is unable to reproduce this characteristic. The difference is that the spectrum of bounded fields in the exponential profile is continuous; thus it is necessary to solve equation (26) to obtain symmetric or antisymmetric modes.

On the other hand, for large values of V the best approximation to the first mode is the parabolic. This is because in this limit the mode is more confined, thus being dominated by behaviour of the profiles in the $|x| < 1$ domain where both cladded-parabolic and parabolic profiles are similar.

The b–V curves for the linear and parabolic approximations have the functional form $b = 1 - V_c/V$, where V_c is the cut-off value for each mode. The remaining curves are more complex. The cut-off values for the first three modes are shown in table 1, where the cut-offs obtained from the series solution are also presented. The parabolic approximation is also called WKB since both give the same dispersion relation. Again, better results are obtained for the hyperbolic secant method.

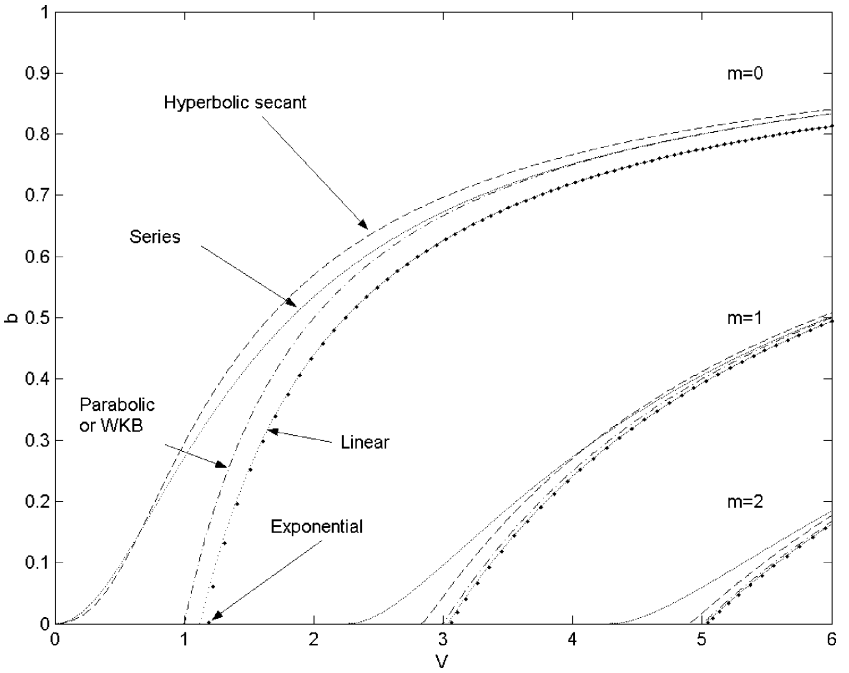

Figure 1. *V–b* plot for the first three modes of the cladded-parabolic profile: (- - -), hyperbolic secant approximation; (———), series solution; (-·-·-), WKB or parabolic approximation; (●), exponential approximation; (· · · · ·), linear approximation.

Table 1. Values of the cut-off V values of the cladded-parabolic profile for the first three modes, as obtained using the methods described in the text. b values for $V = 1.5$ are also given.

	Cut-off V for the first three modes			
Method	$m = 0$	$m = 1$	$m = 2$	b for $V = 1.5$
Series solution	0	2.263	4.287	0.423
Hyperbolic secant	0	2.828	4.899	0.461
Parabolic or WKB	1	3	5	0.333
Linear	1.121	3.035	5.023	0.253
Exponential	1.198	3.062	5.041	0.247

The overall picture that arises from the comparison of these different approximations to the dispersion relation show that only the hyperbolic secant scheme provides a good description of the cladded-parabolic profile. Moreover, parabolic, linear and exponential profiles yield inaccurate values for the fundamental mode cut-off, and more or less similar global results. Here we shall focus our analysis on the fundamental mode. The similarity of the results from the exponential and the linear schemes can be justified in two ways. Firstly, the corresponding profiles are essentially linear for the inner part of the waveguide, so that they yield similar results when the mode is more confined. Secondly, in [9] it has been shown that the linear approximation is a good approximation of the exponential. Thus both profiles have, except for values near the cut-off, a similar capability to approximate a given profile, in this case, the cladded-parabolic profile.

On the other hand, as mentioned above, both linear and parabolic or WKB approximations lead in this example to a dispersion relation of the form $b = 1 - V_c/V$. Therefore differences in the dispersion relations can arise only through the values of the cut-off. In the parabolic approximation, $V = \Lambda$, so that we recover the cut-off of the exact parabolic profile, whose value is one. Moreover, the values of the cut-off in the linear approximation depend only on the solution of the equation (17), or equation (25) in the example analysed here. Both depend on the behaviour of the function $y(x)$ in the centre of the waveguide, explicitly through the derivatives $y''(0)$ and $y'(0)$ and implicitly through the relation between V and Λ. Thus, the ability of the linear approximation to reproduce the dispersion relation is related only to the central portion of problem profile. Since in that portion the cladded parabolic is similar to parabolic, the linear approximation to the cladded parabolic is also the linear approximation to the parabolic profile. Again, in [9] the linear approximation to the purely parabolic profile has been explored, and the cut-off parameters presented there coincide with those in table 1. In conclusion, the inaccuracy of the parabolic approximation in the description of the problem profile arises because both parabolic and cladded-parabolic profiles are the same for $|x| < 1$; the linear approximation fails since it is equal to the approximation to the parabolic profile; finally the exponential approximation yields similar results to the linear approximation except for values near the cut-off.

Now we turn to the analysis of the mode fields. We have constructed the solutions of the fundamental mode for $V = 1.5$ in the region $x \leq 7$ in steps of 0.01 units. The corresponding b values of each approximation are also given in table 1. To this end, it has been necessary to compute the derivative $y'(x)$ in equation (5).

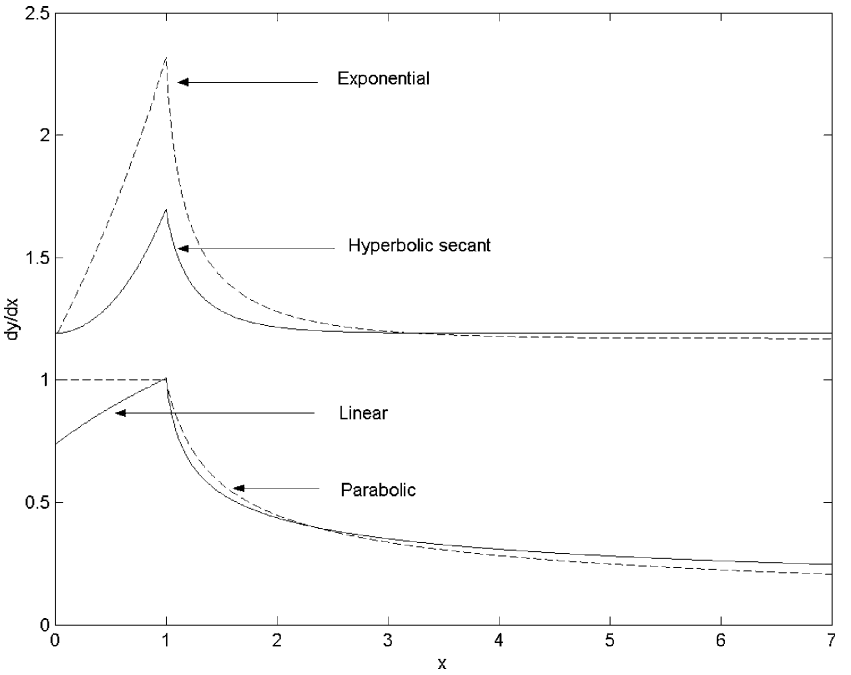

Figure 2. Derivatives of the WKB transformation $y = y(x)$ in the four schemes discussed in the text.

The plot of these derivatives is shown in figure 2. At the turning points, we used the exact limit given in equation (12). These derivatives show where the neglected term in equation (11) is non-zero, which corresponds to domains where the derivative is not constant. The parabolic approximation, for instance, is exact in $|x| < 1$, thus providing a good approximation for confined modes as was justified before.

All the schemes yield smooth solutions as the turning points, contrary to the WKB method. The peak-shaped values at $x = 1$ are due to the change in the definition of the cladded-parabolic profile. Although these peaks imply that the resulting modal fields are not smooth at that point, the overall behaviour of the methods is still acceptable. This is observed in figure 3, where we present the fundamental mode fields E_{HS}, obtained from the hyperbolic secant method, (see equation (19)), together with the series solution from [6]. Both have been normalized so that the total power of the mode is one. The hyperbolic secant has been the best approximation that we have. Note that the discontinuity of the derivative of the field implies that the magnetic field associated with this mode is not well defined in the points where the profile function and so $y'(x)$ are not smooth. This feature is due to the cladded form of the profile, and not to the WKB-type approximation.

Finally, in figure 4 we have plotted the relative accuracy of the hyperbolic secant method, yielding about 10% in the core region. We also observe an increase in the error in the field tail. This is due to the different asymptotic

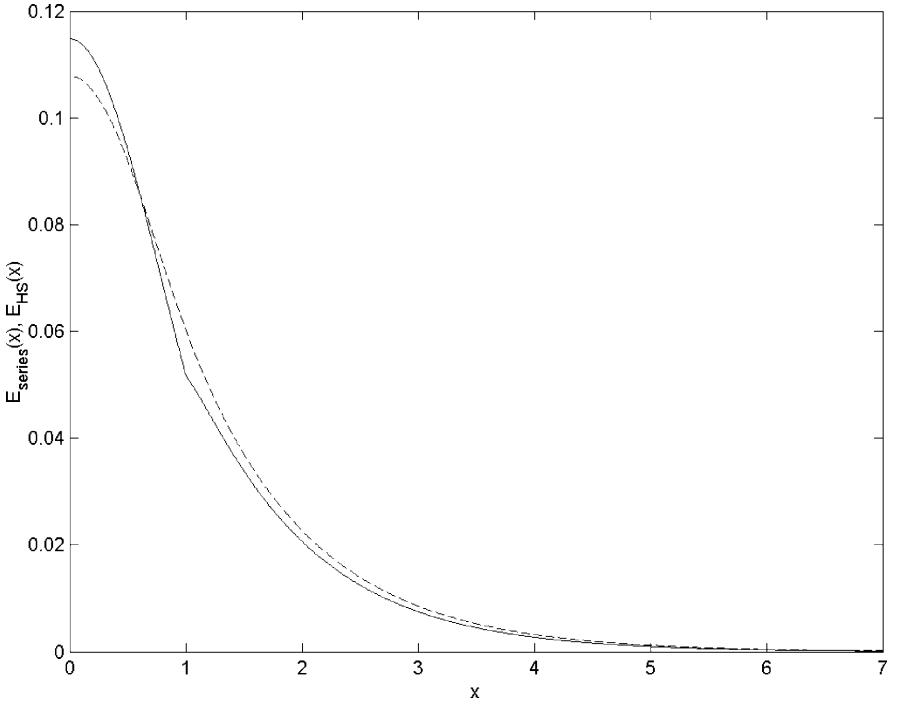

Figure 3. Normalized fundamental mode field of the cladded-parabolic profile corresponding to $V = 1.5$ for the series solution (———) and for the hyperbolic secant WKB method (- - -).

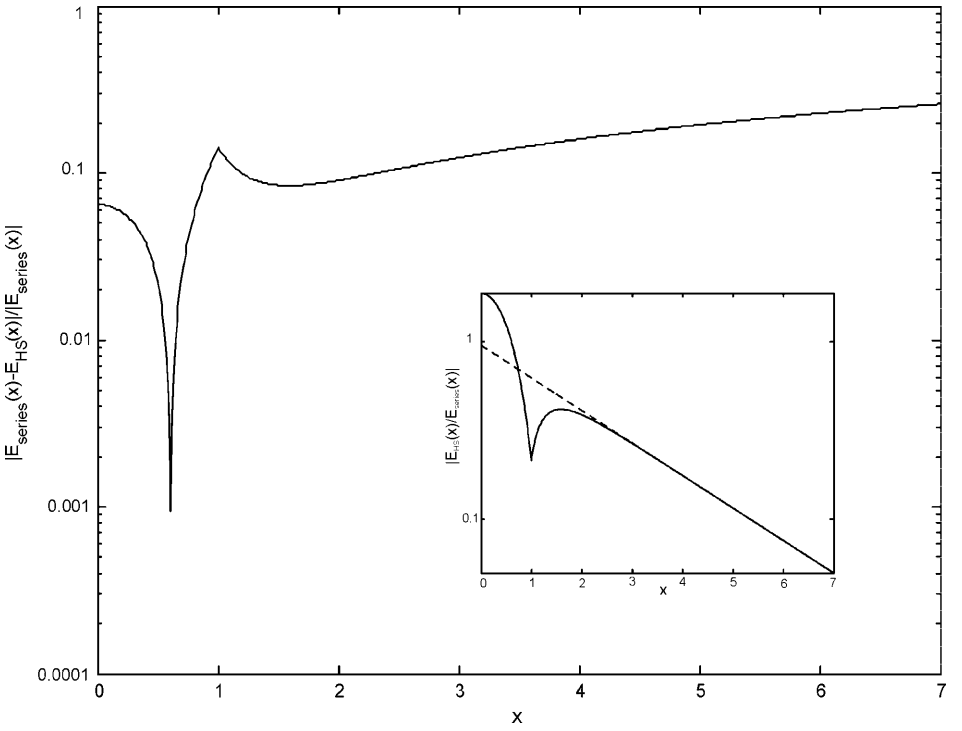

Figure 4. Relative accuracy of the fundamental mode field of the cladded-parabolic profile corresponding to $V = 1.5$ for the hyperbolic secant WKB method compared with the series solution. The inset, shows the asymptotic form and ratio $E_{\mathrm{HS}}/E_{\mathrm{series}}$ on a vertical logarithmic scale.

behaviour of the solutions in the cladding. On the one hand, for large values of x, $E_{\mathrm{HS}}(x) \propto \exp\left[-y(x)\Lambda(b_{\mathrm{HS}})^{1/2}\right]$ from equation (19), where $b_{\mathrm{HS}} = 0.461$ (see table 1). Moreover, $y(x)\Lambda \propto xV$ from equation (7) so that $E_{\mathrm{HS}}(x) \propto \exp\left[-xV(b_{\mathrm{HS}})^{1/2}\right]$. On the other hand, the series solutions for $x > 1$ is $E_{\mathrm{series}}(x) = \exp\left[-xV(b_{\mathrm{ser}})^{1/2}\right]$ with $b_{\mathrm{ser}} = 0.423$. In the inset of figure 4 it is shown this asymptotic form together with the ratio $E_{\mathrm{HS}}/E_{\mathrm{series}}$ as a logarithmic scale.

5. Conclusions

In summary, we have settled in a unified picture several WKB-type methods of analysis of planar waveguides encountered in the literature, adding to these schemes the mapping of a general waveguide into an exponential profile. We have applied them to a non-smooth waveguide, the cladded parabolic, with the result that hyperbolic secant is superior when describing the dispersion relation. On the other hand, results are shown for the fundamental mode field in the hyperbolic secant approximation. The non-smooth character of the index profile results in a discontinuity of the derivative of the modal field, a fact not due to the method itself.

Acknowledgments

This work was supported by the Spanish Ministerio de Ciencia y Tecnologia, under contract TIC-1999-0489. The work of C.R.F.-P. and F.M. has been partially supported by Generalitat Valenciana through project GV01-71.

References

[1] GÓMEZ-REINO, C., PÉREZ, M. V., and BAO, C., 2002, *Gradient-Index Optics: Theory and Applications* (Berlin: Springer).
[2] SCHIFF, L. I., 1955, *Quantum Mechanics* (New York: McGraw-Hill).
[3] MILLER, S. C., and GOOD, R. H., 1953, *Phys. Rev.*, **91,** 174.
[4] KOZAKI, S., OKHI, M., SASAKI, T., SAKURAI, H., and MOTOJIMA, K., 2001, *Appl. Optics*, **40,** 2493.
[5] LANGER, R. E., 1937, *Phys. Rev.*, **51,** 669.
[6] ADAMS, M. J., 1978, *Opt. Quant. Electron.*, **10,** 17.
[7] ADAMS, M. J., 1981, *An Introduction to Optical Waveguides* (CHICHESTER, West Sussex: Wiley).
[8] YATA, A., and IKUNO, H., 1981, *Electron. Lett.*, **17,** 115.
[9] GOYAL, I. C., GALLAWA, R. L., and GHATAK, A. K., 1991, *Jo. Electromagn. Waves and Applic.*, **5,** 623.
[10] GHATAK, A. K., GALLAWA, R. L., and GOYAL, I. C., 1991, *Modified Airy Function and WKB Solutions to the Wave Equation*, NIST MONOGRAPHS, Vol. 176 (Washington, DC: US Government Printing Office).
[11] GALINDO, A., and PASCUAL, P., 1990, *Quantum Mechanics* (Berlin: Springer).
[12] ABRAMOWITZ, M., and STEGUN, I. A., 1964, *Handbook of Mathematical Functions* (New York: Dover Publications).
[13] GÓMEZ-REINO, C., LIÑARES, J., and SOCHACKI, J., 1986, *Appl. Optics*, **25,** 1076.